INSTITUTE OF PHYSICS PUBLISHING PHYSICS IN MEDICINE AND BIOLOGY

Phys. Med. Biol. **51** (2006) 3533–3548 doi:10.1088/0031-9155/51/14/017

Configuration of the electron transport algorithm of PENELOPE to simulate ion chambers

J Sempau[1] **and P Andreo**[2,3]

[1] Institut de Tècniques Energètiques, Universitat Politècnica de Catalunya, Barcelona, Spain
[2] International Atomic Energy Agency, Vienna, Austria
[3] Medical Radiation Physics, University of Stockholm, Karolinska Institute, Stockholm, Sweden

E-mail: josep.sempau@upc.es

Received 27 December 2005, in final form 3 May 2006
Published 6 July 2006
Online at stacks.iop.org/PMB/51/3533

Abstract

The stability of the electron transport algorithm implemented in the Monte Carlo code PENELOPE with respect to variations of its step length is analysed in the context of the simulation of ion chambers used in photon and electron dosimetry. More precisely, the degree of violation of the Fano theorem is quantified (to the 0.1% level) as a function of the simulation parameters that determine the step size. To meet the premises of the theorem, we define an infinite graphite phantom with a cavity delimited by two parallel planes (i.e., a slab) and filled with a 'gas' that has the same composition as graphite but a mass density a thousand-fold smaller. The cavity walls and the gas have identical cross sections, including the density effect associated with inelastic collisions. Electrons with initial kinetic energies equal to 0.01, 0.1, 1, 10 or 20 MeV are generated in the wall and in the gas with a uniform intensity per unit mass. Two configurations, motivated by the design of pancake- and thimble-type chambers, are considered, namely, with the initial direction of emission perpendicular or parallel to the gas–wall interface. This version of the Fano test avoids the need of photon regeneration and the calculation of photon energy absorption coefficients, two ingredients that are common to some alternative definitions of equivalent tests. In order to reduce the number of variables in the analysis, a global new simulation parameter, called the speedup parameter (a), is introduced. It is shown that setting $a = 0.2$, corresponding to values of the usual PENELOPE parameters of `C1` $=$ `C2` $= 0.02$ and values of `WCC` and `WCR` that depend on the initial and absorption energies, is appropriate for maximum tolerances of the order of 0.2% with respect to an analogue, i.e., interaction-by-interaction, simulation of the same problem. The precise values of `WCC` and `WCR` do not seem to be critical to achieve this level of accuracy. The step-size dependence of the absorbed dose is explained in the light of the properties of PENELOPE's transport mechanics. This work is intended to help users to adopt an optimal configuration that guarantees both a high-accuracy calculation of the absorbed dose and a reasonably short computing time.

1. Introduction

The simulation of the response of small ion chambers to photon and electron beams has been, during the last 20 years, one of the most important challenges of the Monte Carlo (MC) simulation of electromagnetic showers. Basically, the difficulty stems from two facts. First, nearly all general-purpose MC codes rely on some form of condensed simulation to transport electrons and positrons. This method, consisting of simulating the effect of a large number of interactions as a single artificial event, is known to produce the so-called interface effects (Bielajew *et al* 1985) when particles move in the vicinity of heterogeneities. These effects can be expected to become more prominent when at least one of the regions adjacent to the interface has a relatively small mass thickness, as is the case with ion chambers. The artefact may manifest as a dependence of the chamber response on the step size adopted in the condensed algorithm.

Second, the cavity is small compared with typical radiation beams used in the clinical practice and, moreover, it is filled with a low density material, usually air. This implies that only a small fraction of the interactions will take place in the air that fills the cavity, thereby leading to inefficient simulations, or equivalently, extremely long computation times. This problem is somewhat less fundamental than the previous one and can be palliated with the use of suitable variance reduction techniques.

A number of papers have been devoted to identifying the origin and assessing the impact of interface effects in high-accuracy dosimetry, both from the point of view of the intrinsic consistency of the algorithm (see, e.g., Smyth (1986), Nahum (1988), Rogers (1993), Foote and Smyth (1995)) and by comparing experimental values with simulations (see Nilsson *et al* (1992) and references therein). The EGS4 code (Nelson *et al* 1985), complemented with the PRESTA algorithm (Bielajew and Rogers 1987), was shown to yield a moderate step-size dependence (Bielajew and Rogers 1988), later considerably reduced with the modifications introduced in PRESTA-II (Bielajew and Kawrakow 1997). The release of EGSnrc (Kawrakow 2000a, 2000b) supplied a tool capable of calculating ion chamber response in a consistent way, in the sense that the results reported were shown to be independent (to within 0.1%) of the electron step length, provided that the user-defined parameters that control this length were kept below certain limits.

The present work studies the consistency, in the same sense as employed before when referring to EGSnrc, of the electron transport algorithm implemented in the PENELOPE code (Salvat *et al* 2003, Sempau *et al* 1997). We have used the version 2003, although the conclusions reached here are expected to remain valid for the recently released version 2005, since the mixed simulation scheme (see below) employed remains basically the same. It is worth mentioning that one of the distinguishing features of this code is the accuracy of the differential cross sections (DCS hereafter) employed for relatively low energies, a characteristic that is particularly relevant for ion chambers since the kinetic energy required by an electron to span the air cavity is of the order of a few keV. For a detailed description of these DCS models, the reader is referred to the PENELOPE manual (Salvat *et al* 2003).

The rest of the paper is organized as follows. First, the basic features of the electron transport scheme adopted in the code are described briefly. In section 3, we propose the use of the so-called Fano theorem to probe, by means of two ideal test cases, the accuracy of this scheme in a way that is pertinent to the simulation of ion chambers. In section 4, a new global simulation parameter is introduced to reduce the dimensionality of the analysis of the stability of the calculated absorbed dose. The obtained results are presented in terms of this parameter in section 5. Some final remarks and conclusions are given in section 6.

2. The PENELOPE mixed algorithm

In this section, we discuss some aspects of the transport scheme of PENELOPE. For electrons (and positrons) this code has recourse to a mixed (or class II, according to Berger (1963)) algorithm in which hard events, defined as those involving angular deflections or energy losses above certain user-defined cutoffs, are simulated in an analogue way, that is, interaction-by-interaction, whereas the combined effect of all the soft ones that occur between two consecutive hard collisions is accounted for by means of a single artificial event. Secondary particles produced as a consequence of soft events are disregarded. The so-called random hinge method, shown to provide accurate values of some relevant angular and spatial moments by Fernández-Varea *et al* (1993), is used to position the artificial event at random along the line determined by the initial position and direction of flight of the particle. The step is truncated whenever an interface separating two different materials is intersected.

The average distance between two consecutive hard interactions, also called the hard mean free path (λ_h), is a non-decreasing function of the mixed simulation cutoffs. Its minimum value corresponds to the mean free path λ between two interactions of any kind and it is reached when all the user-defined cutoffs are set to zero so that artificial soft events are non-existent and the transport is performed in a fully analogue manner[4]. Thus, the algorithm accommodates analogue simulation as a limiting case which the user can select by choosing the appropriate simulation parameters. Note that analogue simulations are named detailed simulations in the PENELOPE documentation.

Since λ_h is a function of the electron energy E, its value is not constant along a step due to the existence of soft collisions. PENELOPE takes this variation into account *exactly* by having recourse to a version of the so-called delta-scattering method which is described in detail in the manual (Salvat *et al* 2003) and that had previously been introduced in EGSnrc (Kawrakow 2000a) with the same aim. One of the consequences of its application is that the resulting step length defined here as the mean distance between two consecutive non-soft stops in the simulation of the electron track[5] is different, in general, from the value of λ_h at the beginning of the step. A consequence of this feature will be commented below.

In principle, longer steps imply faster calculations at the price of sacrificing some accuracy in the description of the transport process since more soft interactions are lumped together into artificial events. In dosimetric applications for which uncertainties of the order of 1% are permissible and interface effects do not play a crucial role (e.g., treatment planning and radiation protection), the configuration of PENELOPE is not critical, as the number of successful applications of the code in various fields indicates (see, e.g., Sempau *et al* (2003)).

For ion chambers, Sempau *et al* (2004) have shown that an appropriate use of analogue simulation in the cavity and its surroundings, thus eliminating the preoccupation for interface effects in this region altogether, leads to results that agree closely with those accepted in the international dosimetric protocols. However, since the individual description of electron interactions in the whole geometry would require a prohibitively large amount of computing time, the region where analogue simulation is applied must necessarily have a limited extension for the calculation to be feasible. The influence of the simulation parameters adopted for the adjacent regions remains unknown and must in principle be studied case by case. The present work provides the insight that permits the prediction of an upper bound for such an effect

[4] In fact, a lower limit for the bremsstrahlung emission cutoff is set internally by PENELOPE at 10 eV to avoid a nonintegrable singularity of the DCS model for a null energy loss. Hence, strictly speaking, bremsstrahlung interactions below 10 eV cannot be described in a completely analogue way with this code.

[5] For readers that are familiar with PENELOPE, this is the distance travelled between three consecutive calls to subroutine KNOCK, the first and the third ones being either hard or delta-scattering events.

and, consequently, the adoption of conservative values for the parameters in question. This knowledge can save a fair amount of CPU time and may avoid the risk of sizeable errors in the calculated doses.

It is remarkable that the combination of mixed simulation and the random hinge circumvents the need to switch to single scattering mode every time the particle approaches an interface or goes away from it. In codes that rely on condensed simulation for *all* elastic collisions this strategy is required if interface effects are to be constrained below acceptable limits, as it has been proven by the success of the EGSnrc code in describing the response of ion chambers. The necessity to switch to single scattering is brought about by the fact that multiple scattering theories underlying condensed-history methods assume that the medium is homogeneous and infinite and, hence, strictly speaking they are not valid if an interface is likely to be reached in a single step. Then, the minimum distance to the surfaces that limit the material object must be calculated as the particle changes its position and this imposes a restriction on the objects that can be modelled efficiently in practice—for a general quadric, for instance, this calculation involves the numerical solution of a sixth-order polynomial equation (Bielajew 1995).

Photons are always simulated in an analogue way, that is, interaction-by-interaction, and therefore the description of their transport relies exclusively on the accuracy of the involved DCSs. Since we shall be concerned only with the performance of the mixed scheme described above, which is responsible for the possible interface effects, the transport of photons has little interest for our analysis and will be ignored.

3. Fano theorem and test cases

The Fano theorem, stated in full and proved by Fano (1954) for the first time, can be expressed in the following terms. Consider an infinite medium in which certain ionizing radiation propagates. For the sake of concreteness, we shall suppose that this radiation is formed of electrons. The medium is assumed to have the same chemical composition and atomic interaction properties (i.e., DCSs) everywhere, although it may have arbitrary mass density variations from point to point. Let us further suppose that an extended source emitting a constant number I of electrons per unit mass is embedded in it, in other words, the volumetric source strength is proportional to the local mass density. The source needs not be isotropic nor monoenergetic. The theorem asserts that, under these circumstances, the angular- and energy-dependent electron fluence is the same everywhere. Since the DCSs are also constant, the absorbed dose D is the same everywhere too. In particular, if the electrons are all generated with an initial energy E_0, the conservation of energy implies

$$D = I E_0 \tag{1}$$

regardless of the local mass density variations and of the DCSs involved.

The premises of the theorem would be met for an ion chamber exposed to an external collimated photon field if photon attenuation in the cavity walls and spatial variations of the DCSs were negligible. In this ideal case, secondary electrons would be generated with a probability per unit volume proportional to the mass density, but this is hardly the case in a real-life experiment. However, as pointed out by Smyth (1986), the Fano conditions can be exactly reproduced in a computer model and this provides a stringent benchmark for condensed-history MC algorithms. Thus, to test the consistency and stability of PENELOPE, a set of fictitious experiments that imitate the conditions found in an ion chamber and that artificially comply with the requirements of the theorem are defined. The deviation of the calculated absorbed dose from the theoretical value given by equation (1) quantifies the adequacy of the mixed

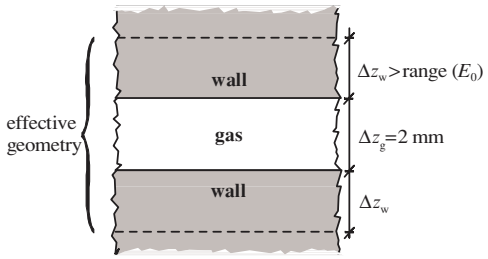

Figure 1. Geometry for the study cases that test the violation of Fano theorem. A 2 mm thick and laterally infinite gas slab is surrounded by infinite solid walls. Electrons of initial energy E_0 are set in motion inside the gas and wall regions, but restricted to the slabs indicated by Δz_w which extend slightly beyond the CSDA range. See the text for details.

simulation scheme. Admittedly, this test does not give any information about the accuracy of the DCS models.

A section of the geometry considered in our simulations is presented in figure 1. An infinite graphite medium with a density of 1.7 g cm^{-3} contains a cavity delimited by two parallel planes (i.e., a slab) that act as the wall interfaces. A fictitious material, which will be referred to as the gas, fills the cavity whose thickness (2 mm) is intended to be representative of a real ion chamber. The gas is identical in composition and DCSs to graphite but with a mass density a thousand-fold smaller. Electrons with initial kinetic energy E_0 equal to 0.01, 0.1, 1, 10 or 20 MeV are generated in the wall and in the gas with a uniform intensity per unit mass I. Two configurations are considered: with the initial direction of emission perpendicular or parallel to the gas–wall interface. These two cases, motivated by the design of pancake- and thimble-type chambers, represent somewhat extreme conditions; a real case, where electrons generated by the impinging photons exhibit a certain angular distribution, constitutes an intermediate situation. As explained before, photons are not essential for our analysis and therefore bremsstrahlung radiation and characteristic x-rays produced by inner shell ionizations are not transported. Secondary (knock-on) electrons will not be followed either. Their contribution is indirectly taken into account by studying the response at different initial energies E_0.

In order to ensure that the wall and the gas have exactly the same atomic interaction properties, the density effect, that is, the variation of the inelastic DCS with the mass density, must be the same in both materials. To this end, the gas is described as if it were solid graphite and the distance that an electron travels between any two consecutive interactions in the cavity is scaled up a thousand-fold. This operation can be readily performed from the user's main program without altering the inner workings of PENELOPE.

The purpose of the simulation is to calculate the dose D absorbed in the gas averaged over a certain cavity volume. More precisely, we shall calculate the quantity Q defined as

$$Q \equiv \frac{D}{I E_0}. \tag{2}$$

Note that, according to the Fano theorem and to energy conservation (cf equation (1)), $Q = 1$ for any *analogue* simulation irrespective of the DCS models implemented in the MC code and of the volume of the gas that is taken as the 'detector'.

Since the planar symmetry of the source and the geometry defined above is bound to propagate to the simulated dose, it is convenient to consider the detector as consisting of a line segment perpendicular to the interface and spanning the cavity. This set-up permits the

application of the reciprocity theorem (Bell and Glasstone 1970) which asserts that the dose absorbed in the detector, normalized to the number of emitted particles, is the same as that obtained in a reciprocal experiment in which the source and the detector have exchanged their respective sections. Here, the section is to be understood as the intersection with a plane parallel to the interface and, thus, it is infinitely large for the original source and infinitely small for the original detector. Therefore, the reciprocal problem involves a line segment source and a detector that covers the whole gas in the cavity, a situation that leads to an efficient (i.e., less time consuming) simulation.

In our case, the reciprocity theorem can be precisely enunciated as follows. If N is the number of simulated particles, the following identity between original and reciprocal simulated quantities holds:

$$\frac{D}{N} \equiv \frac{\Delta E}{N\rho_g A_d \Delta z_g} = \frac{\Delta E'}{N'\rho_g A_s \Delta z_g} \qquad (A_d \to 0, A_s \to \infty), \tag{3}$$

where ΔE is the energy deposited in the detector, Δz_g is the gas thickness, ρ_g is the gas density and A_d and A_s are the detector and source sectional areas, respectively. The symbols $\Delta E'$ and N' refer to the reciprocal situation and the relation $A_s = A'_d$ between the 'original' source area and the reciprocal detector area A'_d has been used in the denominator of the term on the right-hand side of equation (3). Furthermore, the original source intensity I appearing in equation (2) and defined as the number of particles emitted per unit mass reads

$$I = \frac{N}{A_s(2\rho_w \Delta z_w + \rho_g z_g)} \tag{4}$$

with Δz_w and ρ_w being the effective wall thickness (see below) and density, respectively. The factor two accounts for the presence of two walls, one on each side of the cavity. Introducing equation (4) into (2) and using (3) to substitute D/N yields

$$Q = \frac{\Delta E'}{N' E_0}\left(1 + \frac{2\rho_w \Delta z_w}{\rho_g \Delta z_g}\right). \tag{5}$$

This expression involves quantities associated with the reciprocal problem only and hence a finite source, a necessary condition for the simulation to be feasible in practice.

All simulation results are obtained with a statistical relative standard uncertainty (1σ) of 0.05%, except for the 20 MeV cases, obtained with 0.1%. This level of accuracy requires a large amount of computer time. To reduce it range rejection was applied, that is, electrons with a negligible probability of reaching the gas were discarded. To do this, an effective wall thickness Δz_w, depicted in figure 1, was defined such that no particles are generated nor followed beyond this limit. The value of Δz_w was set equal to the CSDA range multiplied by a factor of 1.2 (except for the $E_0 = 0.01$ MeV case for which the factor was 1.4) to take into account the possibility that an electron may travel a distance beyond its CSDA range due to the energy-loss straggling. These factors were obtained from depth–dose curves in graphite by imposing that the contribution to the energy imparted beyond the corresponding extended range is well below 0.1%.

It is interesting to note that our version of the Fano test avoids the need to apply the so-called photon regeneration technique and the calculation of photon energy absorption coefficients. These two ingredients are common to some alternative definitions of the test that rely on a collimated incident photon beam to generate secondary electrons which are subsequently transported in the usual way (see, e.g., Poon *et al* (2005)). Photon regeneration, which consists of resetting photons to their initial state after each interaction, assures a constant I over the ion chamber volume. Photon energy absorption coefficients are necessary to relate the dose to the impinging photon energy fluence and thus obtain the theoretical value of D,

which in our case (cf equation (2)) is obtained by simply invoking energy conservation. An additional advantage of our approach is that the two configurations described above allow a separate analysis of the stability when electrons are set in motion parallel or perpendicular to the interface, whereas electrons produced by a photon beam have a certain angular distribution that causes a mixture of the effects that may occur in the two situations.

4. Simulation parameters

The electron transport algorithm of PENELOPE is determined by six user-defined simulation parameters for each material. These are: an absorption energy (EABS) at which the track evolution is stopped and the kinetic energy of the particle is deposited locally; C1 and C2, which together determine the cutoff angle that separates hard from soft elastic interactions; WCC and WCR, the cutoff energies for the production of hard inelastic and bremsstrahlung events, respectively; and the distance DSMAX, an upper limit to the allowed step length. The reader may consult the PENELOPE manual (Salvat *et al* 2003) for a detailed discussion of the precise definition and physical interpretation of C1 and C2. Except possibly for relatively large values (see below), the step size is a non-decreasing function of all the parameters listed above. As these tend to zero, the description of the transport process becomes more and more detailed. A completely analogue simulation is achieved by setting C1, C2, WCC and WCR equal to zero—see, however, footnote 4.

EABS is usually derived from the experimental arrangement or by the practical requirements of the simulation. For the test cases described in the previous section, the absorption energy for electrons was chosen to be 5 keV, which is about half the kinetic energy of an electron that has a CSDA range equal to the thickness of the gas in the cavity. Photons are not transported, that is, they are absorbed after they are generated (e.g., as bremsstrahlung) by setting the corresponding absorption energy to infinity. In order to ensure a statistically sufficient number of soft interactions in each region, the value of DSMAX should be of the order of one-tenth of the average length of the chord travelled by an electron inside the material in question. Thus, DSMAX in the gas was set to 0.2 mm; the value for the wall is irrelevant since the step length there is already much shorter than one-tenth of the wall effective thickness.

If the four remaining parameters, namely C1, C2, WCC and WCR, are thought of as independent 'variables', the study of the stability of the calculated dose becomes an arduous task. In addition, such general analysis would be of little interest because some combinations are not relevant for ion chamber dosimetry. For instance, large C1 and C2 values combined with small WCC and WCR would describe very accurately the inelastic physics but in a coarse manner the elastic interactions, which is senseless. It is more reasonable to define an overall new simulation parameter on which all the others depend in a convenient manner. The particular form given to this dependence is, of course, somewhat arbitrary. Motivated by this idea, we introduce a new overall parameter a, called speedup parameter hereafter, such that

$$\begin{aligned} \mathtt{C1} &= \mathtt{C2} = a/10 \\ \mathtt{WCC} &= \min\{aE_0/100, \mathtt{EABS}(\mathrm{e}^-)\} \\ \mathtt{WCR} &= \min\{aE_0/1000, \mathtt{EABS}(\gamma)\} \end{aligned} \tag{6}$$

where E_0 is the kinetic energy of the primary particles. Setting $a = 0$ forces all parameters to be null and therefore defines an analogue simulation. The bounds imposed on WCC and WCR by $\mathtt{EABS}(\mathrm{e}^-)$ and $\mathtt{EABS}(\gamma)$, respectively, ensure consistency when secondary particles are followed. The value $a = 1$ is to be considered as the default configuration suitable for most medium-accuracy type of problems. It should also be mentioned that PENELOPE internally limits the maximum values of C1 and C2 to 0.2; no upper limits are set on WCC or WCR.

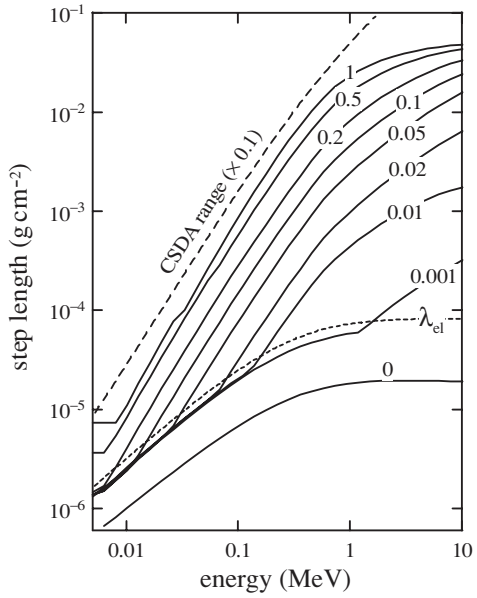

Figure 2. Step length in graphite as a function of the electron kinetic energy (taking $E_0 = 10$ MeV for the purpose of evaluating equations (6)) for different values of the speedup parameter a, indicated by the labels attached to each curve. Note that $a = 0$ represents an analogue simulation. The corresponding minimum step length approximately equals the mean free path λ. The elastic mean free path, λ_{el}, is represented by the dotted line and the CSDA range, scaled down to facilitate the comparison, is the dashed curve.

To help visualize the effect of the simulation parameters on the transport process, it is illustrative to represent the step length s as a function of the kinetic energy for different values of a. This dependence is shown for graphite in figure 2, where it has been assumed that $E_0 = 10$ MeV, $\texttt{EABS}(e^-) = 5$ keV and $\texttt{EABS}(\gamma) = \infty$ in order to obtain WCC and WCR from equations (6). Let us first analyse the variation of s with the energy E. The hard elastic mean free path $\lambda_{h,el}$ and the elastic mean free path λ_{el} decrease continuously with decreasing E (in the considered range), the hard one at a greater rate, that is, with a larger first derivative. As a consequence, the curve $\lambda_{h,el}(E)$ eventually reaches $\lambda_{el}(E)$ as E diminishes and, since the latter is the minimum value of the former, from that point on both quantities coincide. For each a between 0.001 and 0.2, the point at which this happens can be easily identified in the corresponding step length curve because a discontinuity in the first derivative occurs. For $a = 0.5$ and 1, s also shows a discontinuity in the first derivative near $E = 0.01$ MeV, but this time it is produced by the energy-loss correction mechanism based on delta scattering that was mentioned before. This mechanism imposes, for a given a, a minimum step length corresponding to the value of $\lambda_{h,el}$ at the cutoff energy $\texttt{EABS}(e^-) = 5$ keV.

Let us now turn our attention to the variation of s with the speedup parameter a (see figure 2). For $a = 0$, the step length curve reaches a minimum (which is slightly less than the mean free path $\lambda(E)$ because of the effect of the aforementioned energy-loss correction mechanism). As a increases, the hard elastic mean free path increases continuously and so does its contribution to s. The hard inelastic mean free path $\lambda_{h,in}$, on the other hand, is discontinuous with respect to variations of a due to the inelastic DCS model employed, which contains a set of discrete oscillators at fixed energies—the reader may consult the PENELOPE

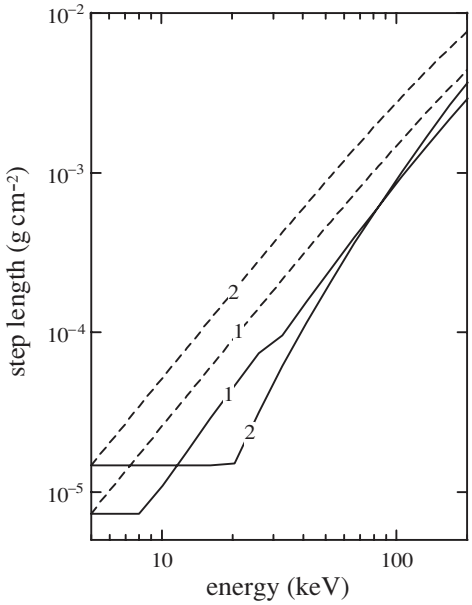

Figure 3. An example of how values of a that are too large can give rise to a decrease of the step length with increasing a. The two solid curves are the step lengths in graphite for $a = 1$ and 2 (see attached labels). Dashed lines are the corresponding hard mean free paths, λ_h, plotted for comparison purposes. The delta-scattering method implemented in PENELOPE to correct for the energy variations along a step is the principal responsible for the difference between the step length and λ_h.

documentation for a detailed description of this model and how the energies of these oscillators are determined. Consequently, $\lambda_{h,in}$ increases suddenly when `WCC` passes above one of the oscillator energies, since the corresponding oscillator ceases to contribute to hard interactions. In particular, graphite is modelled with two oscillators, the lower one located at 21.7 eV approximately. For $a = 0.001$, the value assigned to `WCC` is 100 eV and, therefore, for all the considered a values except zero, the lower oscillator does not contribute to the step length. This fact is responsible for the gap seen between the curves for $a = 0$ and $a = 0.001$. Note also that, as E decreases, the various s curves collapse into a function $f(E)$ that is determined by the combination of λ_{el} and $\lambda_{h,in}$ ('combination' meaning the sum of their inverses), which turns out to be dominated by λ_{el} since $\lambda_{h,in}$ has a much greater value. As a consequence $f(E)$ nearly equals λ_{el}, although not exactly (see figure 2), again because of the energy correction mechanism. The minimum step length ($a = 0$), on the other hand, is determined by the mean free path λ, i.e., by the combination of λ_{el} and λ_{in}. λ is dominated by the inelastic component λ_{in}, which is considerably smaller than λ_{el}.

One feature that deserves some additional comment is the effect of the delta-scattering method employed, as discussed before, to correct for soft energy losses. It turns out that this effect can lead to a *decrease* in the step length for increasing values of a when these are too large. This situation is illustrated in figure 3, where the step length corresponding to two values of the speedup parameter is compared with the corresponding value of λ_h at the beginning of the step, i.e., at the initial energy E, as functions of E. As it can be seen, between 12 and 80 keV, approximately, the step corresponding to $a = 2$ is smaller than that of $a = 1$. This anomaly can be regarded as a warning against the generalized use of simulation parameters

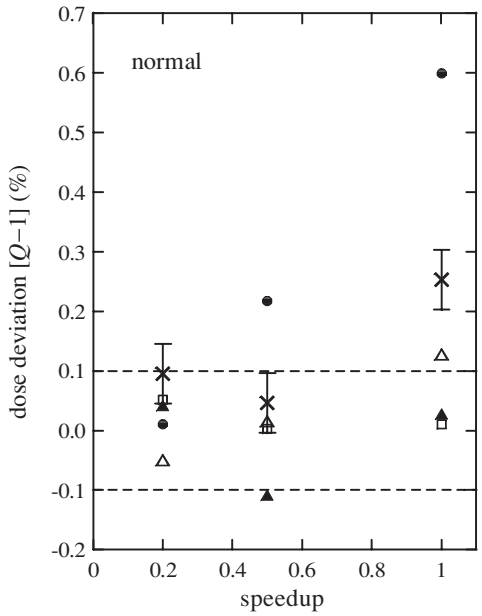

Figure 4. Deviation, in percentage, of the MC calculated dose with respect to the theoretical value as a function of the speedup parameter a. Initially, electrons travel normal to the gas–wall interface with the following kinetic energies: 10 keV (hollow squares), 100 keV (hollow triangles), 1 MeV (dots), 10 MeV (crosses) and 20 MeV (full triangles). All statistical standard uncertainties (1σ) are 0.05% (plotted for the 10 MeV data only) except for the 20 MeV cases for which it is 0.1%. The dashed lines enclose the region where simulation results are compatible with a zero deviation with a confidence level of 95% (68% for the 20 MeV data).

which are too large as it may not only produce a less reliable description of the transport process, but also yield a slower simulation.

5. Discussion

The deviation $(Q - 1)$ in percentage (where Q, given by equation (5), takes the value $Q = 1$ for an analogue simulation, that is, when $a = 0$) for selected values of the speedup parameter a is presented in figures 4 and 5 for the normal and parallel configurations, respectively. The statistical standard uncertainty (1σ) associated with all data points is 0.05% except for the 20 MeV cases, for which it is 0.1%. Dashed lines delimit the region $\pm 0.1\%$ around 0 in which, with a confidence level of 95% (68% for the 20 MeV cases), points should lie in order to be compatible with a zero deviation.

Except in one case (1 MeV, normal), the deviation is of the order of or better than 0.4% even for the largest as analysed. This is a remarkably good result, especially bearing in mind that, as discussed before, in a practical case analogue simulation would be used around the sensitive volume for improved stability and the selected speedup parameter would only be used outside of this region. A much reduced dependency is therefore to be expected in a calculation with a real ion chamber if this prescription is employed. In any case, the setting $a = 0.2$ appears to be low enough to guarantee simulated doses closer than $\sim$0.1% to the true value in the 0.01, 0.1 and 1 MeV cases and in the 10 and 20 MeV normal cases. Larger ($\sim$0.2%–0.4%), but still acceptable deviations for most dosimetric purposes are observed in

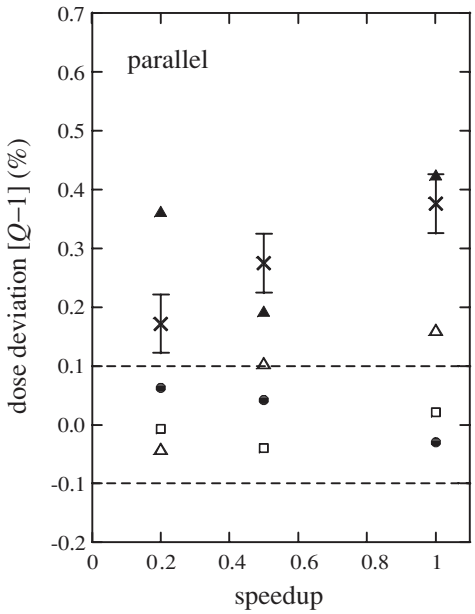

Figure 5. Same details as in figure 4 except that electrons start parallel to the gas–wall interface.

the 10 MeV and 20 MeV parallel cases for the mentioned value of a. Recalling the relation of the simulation parameters with a, (equations (6)), the value suggested for the latter corresponds to C1 = C2 = 0.02 and values of WCC and WCR equal to 0.2% and 0.02% of the initial energy, respectively.

A few selected cases ($E = 100$ keV and 1 MeV both with $a = 0.2$) have been simulated with increased WCCs (5 keV and 100 keV, respectively) without any significant change in the absorbed doses. A similar test has been performed by changing WCR with the same result. This indicates that the dose has little sensitivity to the precise value of the cutoffs WCC and WCR and that it mostly depends on the accuracy with which angular deflections and spatial displacements are described by the transport mechanics of the mixed simulation algorithm. Further support for this assertion can be obtained by calculating the dose when angular deflections are disconnected altogether so that the effect of inelastic physics is made apparent. Note that this is equivalent to assuming that the elastic cross section is zero and that the inelastic DCS does not involve changes of direction of the electron. Since the theoretical dose given by equation (1) does not depend on the particular form of the DCSs, the value of Q for the corresponding analogue simulation continues to be unity. This change in the DCSs can be readily carried out at the main program level by restoring the initial direction of the electron after each interaction. For the 1 MeV case at normal incidence, which involves the largest separation from Fano theorem (see figure 4), the suppression of angular deflections reduces the original deviation of 0.60% down to 0.16%. In the 10 MeV case at normal incidence, the reduction is from 0.25% to 0.10%. In all these cases, the standard uncertainty is ±0.05%. This proves that, at least for the cases analysed, the approximations introduced inherently by the transport mechanics used by the code are responsible for most part of the deviation. These approximations are discussed, among others, by Fernández-Varea *et al* (1993) and Kawrakow and Bielajew (1998).

It is interesting to note that, as it is seen in figures 4 and 5, $Q > 1$ in most cases and, when it is not, the sign of Q is not significant because of its associated uncertainty. In addition, the general trend is that Q increases with a. To justify these results, the following considerations are in order:

- The probability distribution function (PDF) adopted for artificial soft events involving angular deviations (which in PENELOPE is designed to guarantee the correct mean value and variance of the cosine of the angle of deflection for a given path length but is otherwise arbitrary) affects the angular distribution of those electrons that enter the cavity from its close neighbourhood. These particles have not undergone enough artificial soft events (at the hinges) to smear out the details of the artificial PDF, whose higher moments may thus become apparent.
- As shown by Fernández-Varea *et al* (1993), if the transport mechanics of PENELOPE for a given path length s are analysed in the light of the multiple scattering theory of Lewis (1950), and soft energy losses along a step are disregarded, the random hinge scheme *underestimates* the scattering in terms of the penetration depth and of the lateral displacement.
- However, as pointed out by Sempau *et al* (2000), if the energy variation of the transport parameters along a step is taken into account within the framework of Lewis' theory, then the scattering might be *overestimated*.
- When a step is truncated at an interface, a new approximation is introduced. Its effect may depend on a number of factors, including the angle at which the electron was initially travelling with respect to the surface normal.

These observations show the complexity of a theoretical analysis of the remaining dependence of Q on a, even if only an assessment of the tendency (that is, whether the scattering is too weak or too strong) is sought. This analysis is beyond the scope of the present work.

However, a simple numerical experiment can be done easily. To this end, a few energies and path lengths have been selected to determine, by means of MC methods, the trend of the deviation of the scattering angle of the particles entering the cavity. These simulations yielded the following results: (i) globally, the random hinge scheme seems to *overestimate* the mean scattering angle, although the discrepancy is nearly inappreciable after a sufficiently large number of steps, or what is equivalent, for electrons set in motion not very close to the cavity and (ii) this overestimation increases with the step length, that is, with a. These two observations seem to be in accordance with the observed behaviour of Q. A plausible explanation for the sign of $Q - 1$ goes as follows: in the normal case, the overestimation of the scattering implies that electrons reaching the wall–gas interface enter the cavity with an inclination with respect to the surface normal that is too large. This, in turn, leads to an overestimation of the distance travelled inside the gas and, consequently, to an excessive value of the deposited energy. In the parallel case, an increment of the deflection angle involves that more electrons scatter into the cavity, thereby leading again to an increase in the simulated dose. The effect becomes more noticeable for larger values of the speedup parameter.

Simulations performed by Yi *et al* (2006) using a different approach, a different chamber geometry and ^{60}Co gammas showed absorbed dose deviations of the same order of magnitude as ours and a tendency of the simulated dose to increase with the step length, also in agreement with our findings. The sign of the deviation (that is, the equivalent of $Q - 1$), however, was not always positive, although we speculate whether this could be related to the fact that, in one case, their simulation did not converge to the expected theoretical value.

The fluence spectrum in the gas per unit source intensity I is presented in figure 6 for $E_0 = 1$ MeV at normal incidence and two a values, 0.2 and 1. We have selected these two

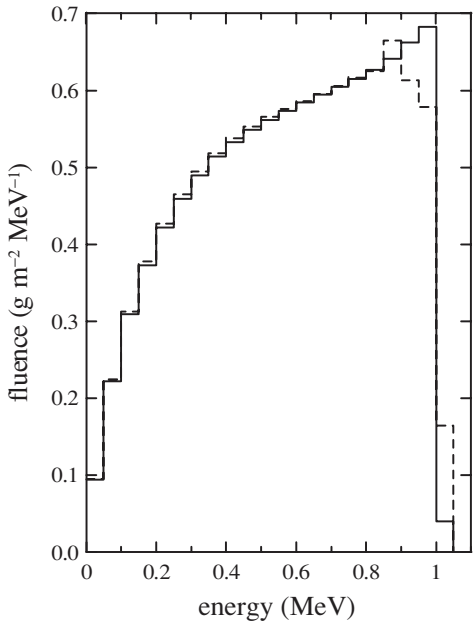

Figure 6. Average fluence spectrum in the gas per unit source intensity I (i.e., per electron generated in 1 g of matter) for the 1 MeV normal case. The solid and dashed histograms correspond to $a = 0.2$ and $a = 1$, respectively.

cases because, based on the calculated absorbed doses (cf figure 4), fluence variations were expected to be more noticeable. This figure serves to show that the fluence obtained with the random hinge mechanism as implemented in PENELOPE is a quantity relatively sensitive to the step length when monoenergetic sources are considered, especially in the high energy end of the spectrum. To illustrate the origin of the discrepancy consider the last bin of the spectrum, which goes from 1 MeV up. In this bin, the track length travelled by electrons that visit the cavity and have not undergone any interaction event, either hard or artificial soft (i.e., a random hinge) and therefore have not lost energy, is accumulated. Greater step lengths involve a longer jump up to the first hinge and therefore a larger probability for an electron born in the wall to reach the cavity with its initial energy intact. This explains the increase in the simulated fluence at 1 MeV for $a = 1$. This increase is compensated by a decrease at the immediately lower energies with the global effect of keeping the absorbed dose, which is related to the integral over energy of the fluence times the restricted stopping power, much less sensitive to a, as figure 4 proves. Likely, the artefact would be much less pronounced, even negligible, for an actual ion chamber, since secondary electrons are then generated with a spectrum of initial kinetic energies and a distribution of initial directions that smear out the contribution of the first and subsequent steps. This assumption is confirmed by the calculations of Yi *et al* (2006) for ^{60}Co gammas.

The variation of the simulation efficiency ϵ, defined in terms of the simulation time t necessary to reach a certain standard uncertainty σ as

$$\epsilon = \frac{1}{t\sigma^2}, \tag{7}$$

is displayed in figure 7 as a function of the speedup parameter a for normal incidence. Note the reduction in simulation time involved even for as as small as 0.2. It must be kept in

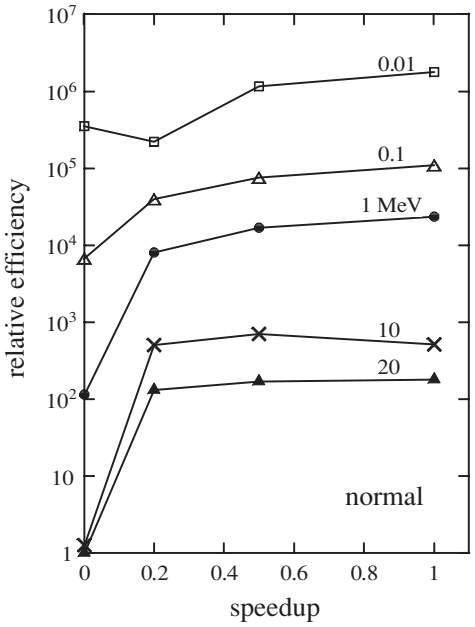

Figure 7. Simulation efficiency as a function of a for the initial energies considered in this work (indicated in MeV) and for normal incidence. Symbols have been joined by straight lines for visual aid. The values presented are relative to the efficiency that yields the simulation of the 20 MeV case with $a = 0$. The absolute efficiency of this latter case is such that, on a cluster with nine AMD K7 XP 1800 processors and using the Intel Fortran Compiler 8.0 for Linux (optimization option '-O'), it would take about 290 days to achieve a 0.1% relative standard uncertainty.

mind, however, that the values found here are valid only for our particular geometry and our simulation methodology. The calculation speed in a real case depends strongly on the actual experimental arrangement, on the use of variance reduction techniques, etc. Apparently, in some cases an increase of a seems to lead to a mild *decrease* in ϵ, although we do not have the elements to assess if this variation is significant or if it is only a statistical deviation due to the (unknown) uncertainty associated with the efficiency. On the other hand, we also speculate that the fact that some soft events have a higher computational cost than their hard counterparts could be at the root of this counterintuitive result.

6. Conclusions

The electron mixed simulation algorithm of PENELOPE has been shown to be consistent with respect to its own cross sections at the sub per cent level for the type of calculations required for high-accuracy dosimetry with ion chambers. The variation of the calculated absorbed doses has been analysed as a function of a new global simulation parameter, the speedup parameter a, related to the usual PENELOPE parameters through equations (6). It has been shown that the setting $a = 0.2$, corresponding to `C1` $=$ `C2` $= 0.02$ and values of `WCC` and `WCR` that depend on the source and absorption energies, is appropriate to obtain tolerances of the order of 0.2% with respect to an analogue simulation of the same problem. The precise values of `WCC` and `WCR` do not seem to be critical to achieve this level of accuracy.

In practice, the flexibility of the mixed simulation scheme of PENELOPE allows the use of analogue simulation, defined by setting $a = 0$, in the chamber cavity and its surroundings. The analysis presented here is therefore applicable for the region adjacent to this inner core. The dependence of the dose on the precise value of a outside the core is likely to be weaker than the variations found in the present work, thus yielding an even more stable algorithm.

Acknowledgments

We would like to thank A Bielajew and F Salvat for many enlightening discussions. One of the authors (JS) acknowledges financial support from the Fondo de Investigación Sanitaria (FIS) of the Spanish Ministerio de Sanidad y Consumo, project no 03/0980.

References

Bell G I and Glasstone S 1970 *Nuclear Reactor Theory* (New York: Van Nostrand-Reinhold)

Berger M J 1963 Monte Carlo calculation of the penetration and diffusion of fast charged particles *Methods in Computational Physics* vol 1, ed B Alder, S Fernbach and M Rotenberg (New York: Academic) pp 135–215

Bielajew A F 1995 HOWFAR and HOWNEAR: geometry modeling for Monte Carlo particle transport *Technical Report* PIRS-0341 (National Research Council of Canada)

Bielajew A F and Kawrakow I 1997 The EGS4/PRESTA-II electron transport algorithm: tests of electron step-size stability *Proc. 12th Conf. on the Use of Computers in Radiation Therapy* ed D D Leavitt and G Starkschall (Madison, WI: Medical Physics Publishing) pp 153–4

Bielajew A F and Rogers D W O 1987 PRESTA: the parameter reduced electron-step transport algorithm for electron Monte Carlo transport *Nucl. Instrum. Methods* B **18** 165–81

Bielajew A F and Rogers D W O 1988 Electron step-size artefacts and PRESTA *Monte Carlo Transport of Electrons and Photons* ed T M Jenkins, W R Nelson, A Rindi, A E Nahum and D W O Rogers (New York: Plenum) pp 115–37

Bielajew A F, Rogers D W O and Nahum A E 1985 The Monte Carlo simulation of ion chamber response to ^{60}Co—resolution of anomalies associated with interfaces *Phys. Med. Biol.* **30** 419–27

Fano U 1954 Note on the Bragg–Gray cavity principle for measuring energy dissipation *Radiat. Res.* **1** 237–40

Fernández-Varea J M, Mayol R, Baró J and Salvat F 1993 On the theory and simulation of multiple elastic scattering of electrons *Nucl. Instrum. Methods* B **73** 447–73

Foote B J and Smyth V G 1995 The modeling of electron multiple-scattering in EGS4/PRESTA and its effect on ionization-chamber response *Nucl. Instrum. Methods* B **100** 22–30

Kawrakow I 2000a Accurate condensed history Monte Carlo simulation of electron transport: I. EGSnrc, the new EGS4 version *Med. Phys.* **27** 485–98

Kawrakow I 2000b Accurate condensed history Monte Carlo simulation of electron transport: II. Application to ion chamber response simulations *Med. Phys.* **27** 499–513

Kawrakow I and Bielajew A F 1998 On the condensed history technique for electron transport *Nucl. Instrum. Methods* B **142** 253–80

Lewis H W 1950 Multiple scattering in an infinite medium *Phys. Rev.* **78** 526–9

Nahum A E 1988 Simulation of dosimeter response and interface effects *Monte Carlo Transport of Electrons and Photons* ed T M Jenkins, W R Nelson, A Rindi, A E Nahum and D W O Rogers (New York: Plenum)

Nelson W R, Hirayama H and Rogers D W O 1985 The EGS4 code system *Technical Report* SLAC-265 (Stanford Linear Accelerator Center)

Nilsson B, Montelius A and Andreo P 1992 A study of interface effects in ^{60}Co beams using a thin-walled parallel plate ionization chamber *Med. Phys.* **19** 1413–21

Poon E, Seuntjens J and Verhaegen F 2005 Consistency test of the electron transport algorithm in the GEANT4 Monte Carlo code *Phys. Med. Biol.* **50** 681–94

Rogers D W O 1993 How accurately can EGS4/PRESTA calculate ion-chamber response? *Med. Phys.* **20** 319–23

Salvat F, Fernández-Varea J M and Sempau J 2003 *PENELOPE: A Code System for Monte Carlo Simulation of Electron and Photon Transport* (Issy-les-Moulineaux, France: OECD Nuclear Energy Agency) Available in pdf format at http://www.nea.fr

Sempau J, Acosta E, Baró J, Fernández-Varea J M and Salvat F 1997 An algorithm for Monte Carlo simulation of coupled electron–photon transport *Nucl. Instrum. Methods* B **132** 377–90

Sempau J, Andreo P, Aldana J, Mazurier J and Salvat F 2004 Electron beam quality correction factors for plane-parallel ionization chambers: Monte Carlo calculations using the PENELOPE system *Phys. Med. Biol.* **49** 4427–44

Sempau J, Fernández-Varea J M, Acosta E and Salvat F 2003 Experimental benchmarks of the Monte Carlo code PENELOPE *Nucl. Instrum. Methods* B **207** 107–23

Sempau J, Wilderman S J and Bielajew A F 2000 DPM, a fast, accurate Monte Carlo code optimized for photon and electron radiotherapy treatment planning dose calculations *Phys. Med. Biol.* **45** 2263–91

Smyth V G 1986 Interface effects in the Monte Carlo simulation of electron tracks *Med. Phys.* **13** 196–200

Yi C-Y, Hah S-H and Yeom M S 2006 Monte Carlo calculation of the ionization chamber response to ^{60}Co beam using PENELOPE *Med. Phys.* **33** 1213–21